Acta Crystallographica Section F
Structural Biology and Crystallization Communications
ISSN 1744-3091

Purification, crystallization and preliminary crystallographic study of a recombinant plant aminoaldehyde dehydrogenase from *Pisum sativum*

Martina Tylichová,[a] Pierre Briozzo,[b] David Kopečný,[a]* Julien Ferrero,[c] Solange Moréra,[c] Nathalie Joly,[b] Jacques Snégaroff[b] and Marek Šebela[a]

[a]Department of Biochemistry, Faculty of Science, Palacký University, Šlechtitelů 11, CZ-78371 Olomouc, Czech Republic, [b]UMR 206 AgroParisTech-INRA de Chimie Biologique, F-78850 Thiverval-Grignon, France, and [c]Laboratoire d'Enzymologie et de Biochimie Structurales, CNRS, F-91198 Gif-sur-Yvette CEDEX, France.

Correspondence e-mail: kopecny_david@yahoo.co.uk

Received 19 November 2007
Accepted 27 December 2007

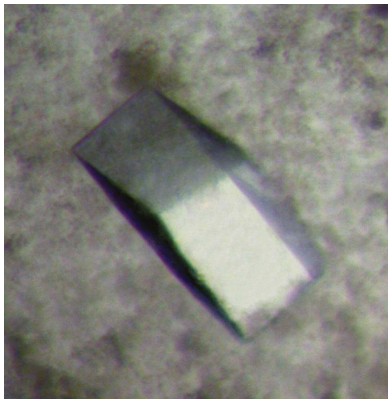

Aminoaldehydes are products of polyamine degradation and are known to be reactive metabolites that are toxic to living cells at high concentrations. These compounds are catabolized by aminoaldehyde dehydrogenases, which are enzymes that contain a nicotinamide adenine dinucleotide coenzyme. Aminoaldehyde dehydrogenase from *Pisum sativum* was overexpressed in *Escherichia coli*, purified and crystallized using the hanging-drop method. A complete data set was collected to 2.8 Å resolution at 100 K. Crystals belong to the monoclinic space group $P2_1$, with unit-cell parameters a = 86.4, b = 216.6, c = 205.4 Å, $\beta = 98.1^\circ$. Molecular replacement was performed and led to the identification of six dimers per asymmetric unit.

1. Introduction

ω-Aminoaldehydes arise from the degradation of polyamines (such as putrescine, spermidine or spermine), which is catalyzed by amine oxidases or polyamine oxidases. The oxidation products (hydrogen peroxide and aminoaldehydes) have been implicated in programmed cell death, induction of cytotoxicity and inhibition of cell division and cause apoptosis in several cell types (Agostinelli *et al.*, 2004). For instance, 3-aminopropionaldehyde (APAL) is considered to be cytotoxic to mammalian cells and causes apoptotic and necrotic death of both neurons and glial cells (Li *et al.*, 2003). Aminoaldehyde dehydrogenases (AMADHs) oxidize various primary ω-aminoaldehydes, namely APAL, 4-aminobutyraldehyde (ABAL) and 4-guanidinobutyraldehyde, to the corresponding ω-amino acids β-alanine, 4-aminobutyric acid and 4-guanidinobutyric acid, respectively. To date, AMADHs have been purified from microorganisms, plants and animals. For historical reasons, they are classified separately as 4-aminobutyraldehyde dehydrogenases (EC 1.2.1.19) and 4-guanidinobutyraldehyde dehydrogenases (EC 1.2.1.54) in the enzyme catalogue (Prieto *et al.*, 1987; Matsuda & Suzuki, 1984). AMADHs contain a nicotinamide adenine dinucleotide (NAD) coenzyme and a reactive cysteine at the active site. According to amino-acid sequence homology, AMADHs are related to betaine aldehyde dehydrogenases (BADHs; EC 1.2.1.8), which are enzymes that mediate the conversion of betaine aldehydes to betaines (Šebela *et al.*, 2000).

In pea (*Pisum sativum*), AMADH is present in two isoforms as demonstrated by activity staining after native gel electrophoresis (Šebela *et al.*, 2001). This was confirmed when two complete cDNAs (AMADH1 and AMADH2) were obtained by 5′ and 3′ RACE-PCR (Brauner *et al.*, 2003). The two 503-amino-acid isoenzymes show 81% sequence identity. The subcellular localization of the pea AMADHs is unknown. Although both isoenzymes carry C-terminal peroxisomal targetting signal type 1 (PTS1), analysis of numerous database-deposited amino-acid sequences or ESTs for plant BADHs and AMADHs suggests the coexistence of peroxisomal and nonperoxisomal isoforms in dicots and monocots (Reumann *et al.*, 2005). In pea root and hypocotyl, most AMADH activity is found in cells belonging to the pericycle and endodermis, while in the epicotyl and shoot apex a major part of the AMADH activity is found in vascular cambium cells (Šebela *et al.*, 2001). The respective roles and localization of

AMADH1 and AMADH2 are not yet known. Native pea AMADH1 shows the highest affinity for APAL and ABAL, while betaine aldehyde is not a substrate. To date, no known three-dimensional structure has been determined of a plant aminoaldehyde dehydrogenase or betaine aldehyde dehydrogenase. Therefore, the structural reason why AMADH1 cannot oxidize betaine aldehyde remains unknown. To gain insight into the substrate specificity, we have purified, crystallized and performed preliminary X-ray diffraction analysis of the recombinant aminoaldehyde dehydrogenase AMADH1 from *P. sativum*.

2. Cloning, expression and purification

The AMADH1 ORF (1510 bp, AJ315852) was cloned into a pET28b His-tag vector (Novagen) digested by *Nde*I and *Xho*I restriction endonucleases. Thus, the primers used for amplification of AMADH1 cDNA contained *Nde*I (upstream primer, 5′-GCTGCATATGG-CAATCACAGTATCAAGT-3′) and *Xho*I (downstream primer, 5′-CGTCTCGAGTATCACAGCTTTGAAGGTGG-3′) restriction sites. The construct was then introduced by heat shock into BL21 Star (DE3) chemically competent *Escherichia coli* cells (Invitrogen) for expression of 6×His-AMADH1. The nucleotide sequence of one selected clone was confirmed by DNA-sequence analysis. For protein expression, transformed BL21 Star (DE3) *E. coli* cells were pre-cultured in Luria–Bertani (LB) medium containing 1% glucose and kanamycin (30 µg ml^{-1}) at 310 K overnight. Cells were harvested by centrifugation at 4000*g* for 5 min and then grown in LB medium containing kanamycin (30 µg ml^{-1}) to an OD_{600} of about 0.6. AMADH1 expression was induced with 0.1 m*M* isopropyl *β*-D-1-thiogalactopyranoside (IPTG) and the culture was incubated at 293 K overnight. After induction, cells were harvested by centrifugation at 5000*g* for 10 min and stored frozen.

Cells were resuspended in a lysis buffer containing 50 m*M* Tris–HCl pH 8.0, 10 m*M* $MgCl_2$ and one tablet of EDTA-free protease inhibitors (Roche) followed by the addition of lysozyme (0.3 mg ml^{-1}). After 1 h incubation at room temperature, 1%(*w*/*v*) Triton X-100, RNAse (0.01 µg ml^{-1}) and DNAse (0.04 U µl^{-1}) were added. Finally, after 30 min incubation at 310 K, 100 m*M* NaCl and 5%(*w*/*v*) glycerol were added. The lysate was then centrifuged at 12 000*g* for 30 min and the supernatant containing expressed 6×His-AMADH1 was recovered.

The supernatant was loaded onto a column packed with His-selected cobalt gel (Sigma) equilibrated with 20 m*M* Tris–HCl buffer pH 8.0 containing 100 m*M* NaCl, 10 m*M* imidazole and 5% glycerol. Elution was performed using 250 m*M* imidazole in the same buffer. Pure AMADH1 was concentrated using 30 kDa cutoff filters (Centricon). The total yield of purified AMADH1 was about 6 mg per litre of culture medium. The enzyme was characterized by a specific activity value of 2.7 µmol s^{-1} mg^{-1} measured by monitoring NADH formation at 340 nm using APAL as a substrate (Šebela *et al.*, 2000). To confirm the purity and correct expression of AMADH1, SDS–PAGE was performed using the Nu-PAGE system from Invitrogen. After electrophoresis, the protein bands were visualized by Coomassie staining (CBB G-250), Western blotted and detected using AMADH antibodies (Fig. 1*a*). The experimental molecular weight of 57 kDa and also the pI of 5.8 (as obtained by isoelectric focusing; not shown) of recombinant AMADH1 were both in agreement with calculated values. MALDI–TOF peptide mass fingerprinting of AMADH1 after in-gel digestion of a 5 pmol sample (Šebela *et al.*, 2006) allowed unambiguous identification in the MSDB database (accession No. Q8VWZ1). The identified 21 peptides covered 51% of the sequence and matched with an accuracy of 18 p.p.m.; the probability-based MOWSE score was 266.

3. Crystallization

Prior to crystallization, the enzyme was desalted and concentrated to 18 mg ml^{-1} by ultrafiltration using a Centricon 30 kDa cutoff device (Amicon). Crystals were grown at 293 K using the hanging-drop vapour-diffusion method. Preliminary crystallization conditions were found using a screening kit (Crystal Screen, Hampton Research). Small crystals appeared within two weeks using condition No. 48 from Crystal Screen 2. Crystallization conditions were then optimized. 2 µl AMADH1 solution with 10 m*M* NAD (Sigma–Aldrich) was mixed with 2 µl of a reservoir solution containing 0.1 *M* HEPES pH 7.5, 13%(*w*/*v*) PEG 6000 and 5%(*v*/*v*) 2-methyl-2,4-pentanediol, leading to both transparent clustered and a few good single crystals (Fig. 1*b*).

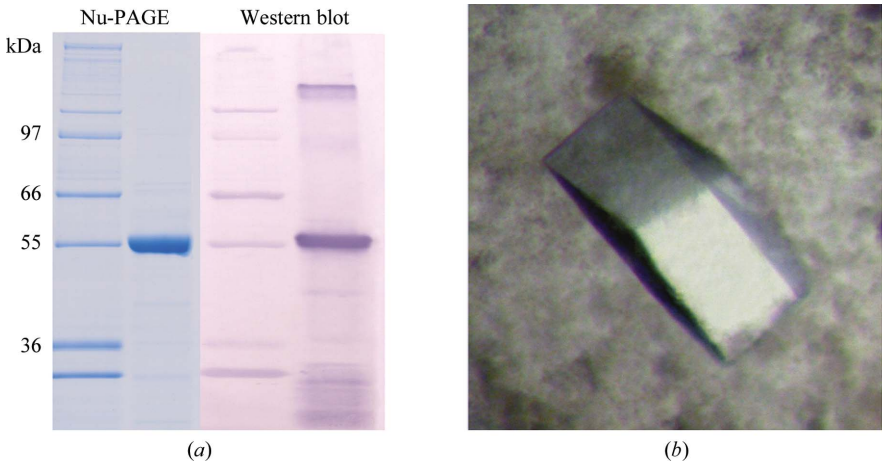

Figure 1
(*a*) Nu-PAGE and Western blot of a recombinant pea aminoaldehyde dehydrogenase (AMADH1). Nu-PAGE was performed using 4–12% bis-tris gel in MOPS buffer. The PVDF membrane was probed with polyclonal anti-AMADH rabbit antibodies, reacted with goat anti-rabbit IgG alkaline phosphatase conjugate and coloured using NBT/BCIP (nitro blue tetrazolium chloride/5-bromo-4-chloro-3-indolyl phosphate, Roche). (*b*) Crystals of AMADH1. The crystal shown (maximum dimension 0.3 mm) is similar to that used for the X-ray diffraction data collection.

Table 1
Data-collection statistics.

Values in parentheses are for the highest resolution shell.

Space group	$P2_1$
Unit-cell parameters (Å, °)	a = 86.4, b = 216.6, c = 205.4, β = 98.1
Resolution (Å)	30.0–2.8 (2.95–2.8)
No. of observed reflections	2130930
No. of unique reflections	178951
Completeness (%)	97.8 (93.1)
$R_{\rm merge}$† (%)	13.7 (42.9)
$\langle I\rangle/\langle\sigma(I)\rangle$	7.7 (2.0)

† $R_{\rm merge} = \sum_{hkl}\sum_i |I_i(hkl) - \overline{I(hkl)}|/\sum_{hkl}\sum_i I_i(hkl)$, where $I_i(hkl)$ is the intensity of an observation and $\overline{I(hkl)}$ is the mean value of its unique reflection; the summations are over all reflections.

4. Data collection and processing

Crystals were soaked in a cryoprotectant solution (reservoir solution supplemented with 20% glycerol) for 3 min and flash-frozen in liquid nitrogen. Data-collection experiments were carried out at 100 K on the ID14-3 beamline at the European Synchrotron Radiation Facility (Grenoble, France) equipped with an ADSC Q4 CCD detector and tuned to 0.93 Å wavelength. 260° of data were collected in 1° frames, with 5 s exposure per frame. Diffraction intensities were evaluated using the program *MOSFLM* (Leslie, 1992). Data were further processed to 2.8 Å resolution using the *CCP*4 program suite (Collaborative Computational Project, Number 4, 1994). The crystal belongs to the monoclinic space group $P2_1$, with unit-cell parameters a = 86.4, b = 216.6, c = 205.4 Å, β = 98,1°. Data-collection and processing statistics are given in Table 1.

5. Molecular replacement

A search for a sequence-related protein of known crystal structure using the program *PHYRE* (the successor to 3*D-PSSM*; Kelley *et al.*, 2000) indicated several proteins with secondary structure similar to that predicted for AMADH1. All belong to the aldehyde dehydrogenase (ALDH) superfamily and have sequence identities of up to 41% (human and bovine mitochondrial ALDHs and cod liver BADH). Most of the AMADH or ABALDH (4-aminobutyraldehyde dehydrogenase) enzymes have been reported to be homotetramers. The asymmetric unit can contain three or four tetramers, corresponding to Matthews coefficients (Matthews, 1968) of 2.78 and 2.09 Å^3 Da^{-1}, respectively. However, attempts to use molecular replacement to solve the structure of AMADH1 with the program *Phaser* (Storoni *et al.*, 2004) gave no solution for three tetramers using the tetrameric structure of human mitochondrial ALDH (PDB code 1cw3) as a model search. When the monomer was used as a model, 12 monomers were placed in the asymmetric unit by the program. Examination of the resulting model showed that the 12 monomers form six dimers, suggesting that the active form of AMADH1 in solution is a dimer, similar to the case for a few ABALDH enzymes. Assuming that the unit cell contains six dimers per asymmetric unit, the calculated Matthews coefficient is 2.78 Å^3 Da^{-1}, corresponding to a solvent content of 55.8%. Refinement of the complete AMADH1 structure is under way.

This work was supported by grants MSM 6198959215 and MSM 6198959216 from the Ministry of Education, Youth and Sports of the Czech Republic. We thank the staff of ESRF in Grenoble for making station ID14-3 available.

References

Agostinelli, E., Arancia, G., Dalla Vedova, L., Belli, F., Marra, M., Salvi, M. & Toninello, A. (2004). *Amino Acids*, **27**, 347–358.
Brauner, F., Šebela, M., Snégaroff, J., Peč, P. & Meunier, J. C. (2003). *Plant Physiol. Biochem.* **41**, 1–10.
Collaborative Computational Project, Number 4 (1994). *Acta Cryst.* D**50**, 760–763.
Kelley, L. A., MacCallum, R. M. & Sternberg, M. J. E. (2000). *J. Mol. Biol.* **299**, 499–520.
Leslie, A. G. W. (1992). *Jnt CCP4/ESF–EACBM Newsl. Protein Crystallogr.* **26**.
Li, W., Yuan, X. M., Ivanova, S., Tracey, K. J., Eaton, J. W. & Brunk, U. T. (2003). *Biochem. J.* **371**, 429–436.
Matsuda, H. & Suzuki, Y. (1984). *Plant Physiol.* **76**, 654–657.
Matthews, B. W. (1968). *J. Mol. Biol.* **33**, 491–497.
Prieto, M. I., Martin, J., Balaña-Fouce, R. & Garrido-Pertierra, A. (1987). *Biochimie*, **69**, 1161–1168.
Reumann, S., Ma, C., Lemke, S. & Babujee, L. (2005). *Plant Physiol.* **136**, 2587–2608.
Šebela, M., Brauner, F., Radová, A., Jacobsen, S., Havliš, J., Galuszka, P. & Peč, P. (2000). *Biochim. Biophys. Acta*, **1480**, 329–341.
Šebela, M., Luhová, L., Brauner, F., Galuszka, P., Radová, A. & Peč, P. (2001). *Plant Physiol. Biochem.* **39**, 831–839.
Šebela, M., Štosová, T., Havliš, J., Wielsch, N., Thomas, H., Zdráhal, Z. & Shevchenko, A. (2006). *Proteomics*, **6**, 2959–2963.
Storoni, L. C., McCoy, A. J. & Read, R. J. (2004). *Acta Cryst.* D**60**, 432–438.